Int J Clin Exp Med 2015;8(1):625-633
www.ijcem.com /ISSN:1940-5901/IJCEM0003913

Original Article

Protein expression of phospho-lim kinase-1 in patients and an experimental rat model with intractable temporal lobe epilepsy

Hao Huang[1], Heng Wang[1], Jinxian Yuan[1], Xuling Wu[1], Yunyi Huang[1], Xin Zhou[1], Yangmei Chen[1]

[1]*Department of Neurology, Second Affiliated Hospital of Chongqing Medical University, 74 Lin Jiang Road, Chongqing 400010, China*

Received November 17, 2014; Accepted January 9, 2015; Epub January 15, 2015; Published January 30, 2015

Abstract: Lim kinase-1 (LIMK1) plays a critical role in dendritic spine morphogenesis and brain function. The protein expression pattern of phospho-LIMK1 (p-LIMK1), the active form of LIMK1, in intractable temporal lobe epilepsy (TLE), however, is unknown. Here we measured p-LIMK1 protein expression in thirty temporal neocortex tissue samples from intractable TLE patients, fifteen histologically normal temporal neocortex tissue samples from trauma patients without epilepsy, in the hippocampi of lithium chloride/pilocarpine-induced TLE rats, and in controls. We found that p-LIMK1 was expressed mainly in the cytoplasm of neurons. The protein expression of p-LIMK1 was significantly higher in the TLE patients and rats than in the control groups. Our results suggest that p-LIMK1 might be involved in the pathogenesis of intractable TLE.

Keywords: Lim kinase-1, phospho-LIMK1, intractable temporal lobe epilepsy, lithium chloride, pilocarpine

Introduction

Epilepsy is characterized by recurrent spontaneous seizures. Of the epilepsy patients receiving anti-epileptic drugs (AEDs), 20-30% still have seizures and most of them will progress to intractable temporal lobe epilepsy (TLE) [1]. The pathogenesis of intractable TLE, however, is still unclear.

Abnormalities in dendritic spines, axons and synaptic plasticity have commonly been observed in brain specimens from epilepsy patients and epileptic animal models [2-5]. Interestingly, Lim kinase-1 (LIMK1) plays a critical role in dendritic spine morphogenesis and brain function. LIMK1 is a cytoplasmic serine/threonine kinase expressed in neurons of the central nervous system (CNS) [6]. Phospho-LIMK1 (p-LIMK1) is an active form of LIMK1 that is phosphorylated at the site of threonine 508 by Rho GTPases [7, 8]. Meanwhile, p-LIMK1 phosphorylates and thus inactivates cofilin and actin-depolymerizing factor (ADF), which are key regulators of actin cytoskeleton dynamics that have been implicated in growth cone motility and neurite extension [9]. Extensive evidence has shown that LIMK1 is important to increase the number of dendritic spines, stimulate the growth of axons and dendrites [10], sustain mature synapses [11] and change the hippocampal long-term potentiation (LTP) [12]. Thus, we hypothesized that p-LIMK1 might participate in the pathogenesis of TLE. This study was designed to determine the expression pattern of p-LIMK1 in intractable TLE patients and in experimental TLE rats.

Materials and methods

Patients

In this study, thirty human brain samples were selected randomly from our epilepsy brain bank, which consists of 300 brain samples from patients with intractable TLE who were refractory to the maximal doses of three or more AEDs including valproic acid, phenobarbital, phenytoin, carbamazepine, clonazepam, topiramate, lamotrigine, oxcarbazepine, and gabapentin. All patients had typical clinical manifestations and characteristic electroen-

Table 1. Clinical features of the TLE patients

No.	Sex	Age (years)	Duration (years)	Seizure type	AEDs	Resected tissue	Pathology
1	F	25	8	SGS, SPS	CBZ, VPA, PB	TNR	g, nl, nd
2	F	19	15	GTCS	VPA, CBZ, PHT	TNL	g, nl, nd
3	M	15	7	SGS	CBZ, PHT, VPA	TNL	g, nl
4	F	59	20	CPS	CBZ, PHT, VPA, CBL	TNR	g, nl, nd
5	M	14	4	SPS, SGS	CBZ, VPA, CBL	TNL	g, nl
6	M	5	2	CPS	OXC, CBL, VPA, TMP	TNL	g, nl
7	F	9	4	CPS	OXC, VPA, GBP	TNR	g, nl
8	M	22	4	SPS, SGS	CBZ, VPA, PHT	TNR	g, nl, nd
9	M	39	16	CPS, SGS	CBZ, VPA, TPM	TNR	g, nl, nd
10	F	20	8	GTCS	VPA, CBZ, PHT	TNL	g
11	M	23	7	SGS	CBZ, PHT, TPM	TNL	g, nl, nd
12	F	39	17	CPS, SGS	CBZ, VPA, CBL, TPM	TNL	g, nl, nd
13	M	20	11	SGS	CBZ, VPA, TPM	TNR	g, nl
14	M	37	9	CPS, SGS	CBZ, VPA, PHT	TNL	g, nl, nd
15	F	25	12	CPS, GTCS	CBZ, PHT, VPA, TMP	TNR	g, nl
16	F	4	2	SPS	OXC, PHT, TMP	TNR	g, nl
17	M	14	6	CPS	OXC, VPA, LTG	TNL	g, nl
18	M	33	8	SGS	CBZ, PHT, LTG	TNR	g, nl, nd
19	M	27	5	CPS, SGS	CBZ, PHT, LTG, CBL	TNR	g, nl
20	F	17	6	SPS	CBZ, PHT, TMP	TNL	g, nl
21	F	29	17	CPS, SGS	CBZ, PHT, VPA, LTG	TNR	g, nl, nd
22	M	4	3	GTCS	VPA, OXC, PHT, TMP	TNR	g
23	F	44	8	CPS	CBZ, VPA, LTG	TNR	g, nl, nd
24	M	52	18	CPS, SGS	CBZ, PHT, TMP, CBL	TNL	g, nl, nd
25	F	48	14	CPS	CBZ, PHT, TMP	TNL	g, nl, nd
26	M	33	10	SGS	CBZ, VPA, LTG	TNR	g, nl
27	M	28	12	SGS	CBZ, VPA, LTG, PHT	TNR	g, nl, nd
28	F	45	12	CPS, SGS	CBZ, VPA, CBL, TMP	TNL	g, nl, nd
29	M	44	20	CPS, SGS	CBZ, VPA, LTG, TMP	TNL	g, nl, nd
30	F	15	8	CPS, SGS	CBZ, VPA, CBL	TNR	g, nl

Sex: *F,* female; *M,* male. Seizure type: *CPS,* complex partial seizure; *GTCS,* generalized tonic-clonic seizure; *SGS,* secondarily generalized seizure; *SPS,* simplex partial seizure. AEDs, anti-epileptic drugs: *CBZ,* carbamazepine; *CLB,* clonazepam; *GBP,* gabapentin; *LTG,* lamotrigine; *OXC,* oxcarbazepine; *PB,* phenobarbital; *PHT,* phenytoin; *TPM,* topiramate; *VPA,* valproic acid. Resected tissue: *TNL,* left temporal neocortex; *TNR,* right temporal neocortex. Pathology: *nl,* neuronal loss; *nd,* neuronal degeneration; *g,* gliosis.

cephalograms (EEGs). The diagnosis of seizure types was based on the 1981 International Classification of Epilepsy Seizures of the International League Against Epilepsy. Prior to the resection of temporal lobe tissue, patients were subjected to pre-surgical assessments consisting of the historic details of seizures, neurological examination, interictal and ictal EEG studies, neuroradiological studies, and neuropsychological tests. The epileptic lesion was localized in each patient through brain magnetic resonance imaging (MRI) or computed tomography (CT), 24-h EEG or video EEG, sphenoidal electrode monitoring or intraoperative electrocorticography. Furthermore, the related laboratory tests did not show any other nervous system diseases or progressive lesions in the CNS. After the resection of temporal lobe lesion tissue, the electrodes for intraoperative electrocorticography were placed on the remaining edge of tissue to ensure that the lesion was resected completely. The pathological findings in the resected tissue included gliosis, neuronal loss and neuronal degeneration. **Table 1** summarizes the clinical features of the intractable TLE patients.

For comparison, fifteen histologically normal temporal neocortex samples were obtained from patients who had required surgery because of severe brain trauma. All of these patients were diagnosed by licensed pathologists as brain trauma and had no prior history of seizures, exposure to AEDs, or other neurologic disorders. Two neurologists reviewed all of the medical records of these patients and none of them developed epilepsy after the trauma. **Table 2** shows the clinical features of the control group of patients.

Informed consents were obtained from all patients or their guardians for the surgery treatment and for the use of brain tissue for research purposes. The protocol of this study complied

Table 2. Clinical features of the 15 patients in the control group

Sex	Age (years)	Etiology diagnosis	Resected tissue	Adjacent tissue pathology
F	20	Trauma	TNL	Normal
F	23	Trauma	TNR	Normal
M	30	Trauma	TN	Normal
M	19	Trauma	TNR	Normal
M	21	Trauma	TNL	Normal
F	49	Trauma	TN	Normal
M	16	Trauma	TNL	Normal
F	47	Trauma	TNR	Normal
M	14	Trauma	TNL	Normal
F	50	Trauma	TN	Normal
F	33	Trauma	TNL	Normal
M	24	Trauma	TN	Normal
M	18	Trauma	TNL	Normal
F	21	Trauma	TNR	Normal
M	17	Trauma	TNL	Normal

Sex: *F,* female; *M,* male. Resected tissue: *TNL,* left temporal neocortex; *TNR,* right temporal neocortex.

with the guidelines for the conduct of research involving human subjects as established by the National Institutes of Health and the Committee on Human Research at Chongqing Medical University. The research was performed in accordance with the Declaration of Helsinki of the World Medical Association.

A rat model of TLE

Forty six adult male Sprague-Dawley rats, aged 8 weeks and weighing 180-220 g, were obtained from the Experimental Animal Center of Chongqing Medical University. All experimental procedures were performed in accordance with the guidelines of the Animal Care Committee and the Ethical Commission of Chongqing Medical University. Rats were randomly divided into eight groups, including one control group and seven epilepsy-induced subgroups stratified by the period of time since seizure: 1/4, 1, 3, 7, 14, 30, and 60 days (n = 8 in the control and 60-day groups; n = 5 in the remaining subgroups). TLE rats were induced by lithium chloride (LiCl, 127 mg/kg, Sigma-Aldrich, USA) and pilocarpine (50 mg/kg, Sigma-Aldrich) according to the refractory TLE model [13]. The control rats were treated with normal saline, instead of pilocarpine. The rats with continuous generalized tonic seizures at stages 4 or 5 according to Racine's standard criteria [14], but without normal behavior between seizures, were defined as status epilepticus and were included in the study of acute period of TLE. A video recording system was used to monitor the spontaneous recurrent seizures of the model rats in chronic period of TLE (12 h/day, for 3 days). Those rats with spontaneous recurrent seizures in chronic period were also included in the study. The induced epileptic rats were sacrificed at 1/4, 1, 3, 7, 14, 30, and 60 days after seizures, while the control group of rats were sacrificed at day 1, and the brain tissues were removed for analysis.

Tissue processing

All human brain tissues and the bilateral hippocampus of forty rats (5 per group) were divided into two portions. One portion was immediately stored in liquid nitrogen for Western blot assay. The other portion was fixed in 4% paraformaldehyde and embedded in paraffin for immunohistochemistry and terminal deoxynucleotydyl transferase mediated dUTP nick-end-labeling (TUNEL) staining. The remaining six rat brains from the control and 60-day groups (3 per group) were selected for visualization of the dendrite morphology by Golgi staining.

Immunohistochemistry

Primary polyclonal rabbit anti-p-LIMK1 antibody (1:100, Abcam, USA) was used for detecting the immunoreactivity of p-LIMK1 by immunohistochemistry [15]. Neurons with buffy staining in the cytoplasm were defined as positive for p-LIMK1. Ten visual fields of every section were chosen randomly under the LEICA DM6000B automatic microscope, and the optical density (OD) values of immunoreactivity were analyzed automatically and semi-quantitatively using Image Pro-Plus 6.0 pathology image analysis system.

Western blot analysis

Total protein were separated by 10% SDS-PAGE and electrotransferred to PVDF membranes. The membranes were incubated with primary polyclonal rabbit anti-LIMK1 (1:100, Santa Cruz, USA), anti-p-LIMK1 (1:50, Abcam), or anti-β-actin antibody (1:1000, Santa Cruz) at 4°C overnight. The membranes were washed and then incubated with an HRP-labeled goat anti-rabbit secondary antibody (1:4000, Zhongshan Golden Bridge, Inc.). The immunoreactive

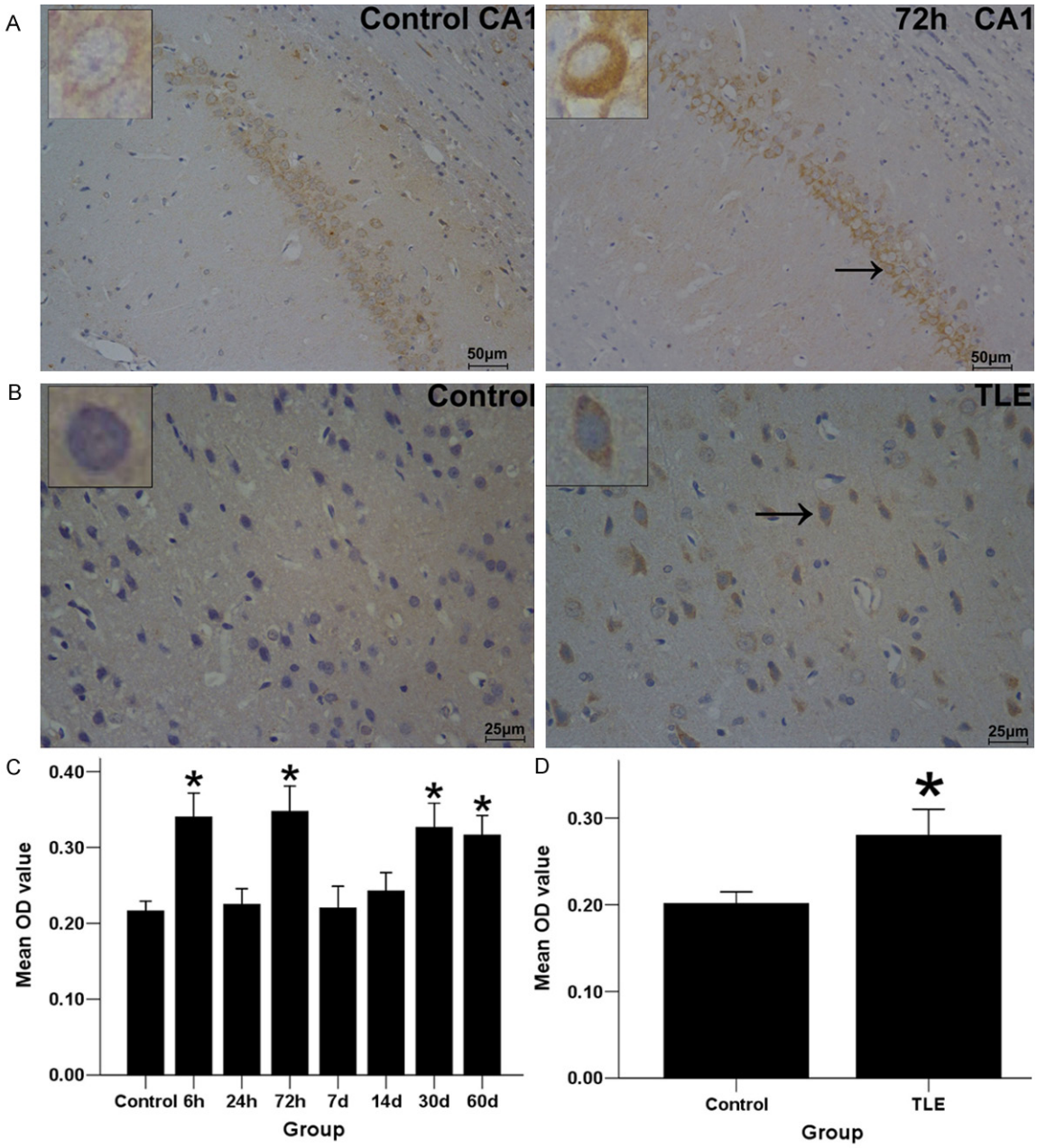

Figure 1. Expression of p-LIMK1 was measured by immunohistochemistry. The p-LIMK1-positive neurons in the CA1 region of TLE rat hippocampi (A), and in the temporal neocortexes of TLE patients (B). The p-LIMK1 immunoreactivity in the CA1 region of rat hippocampi compared between TLE rat subgroups (n = 5) and control group (n = 5) (C), and in the temporal neocortex compared between TLE patients (n = 30) and controls (n = 15) (D). *$P < 0.05$ versus control. The black arrows indicate p-LIMK1-positive neurons.

bands were detected using a chemiluminescent substrate (Pierce, USA). The OD value of each protein band was visualized and quantified using a LICOR Odyssey Infrared Imaging System (LICOR Bioscience, USA). Then the OD value of p-LIMK1 was normalized to that of β-actin.

TUNEL staining

An apoptosis kit (Roche, Schweiz) was used for detecting apoptotic neurons in patients [16]. Neurons with buffy staining in the nucleus were defined as apoptotic neurons. The average numbers of apoptotic neurons were determined

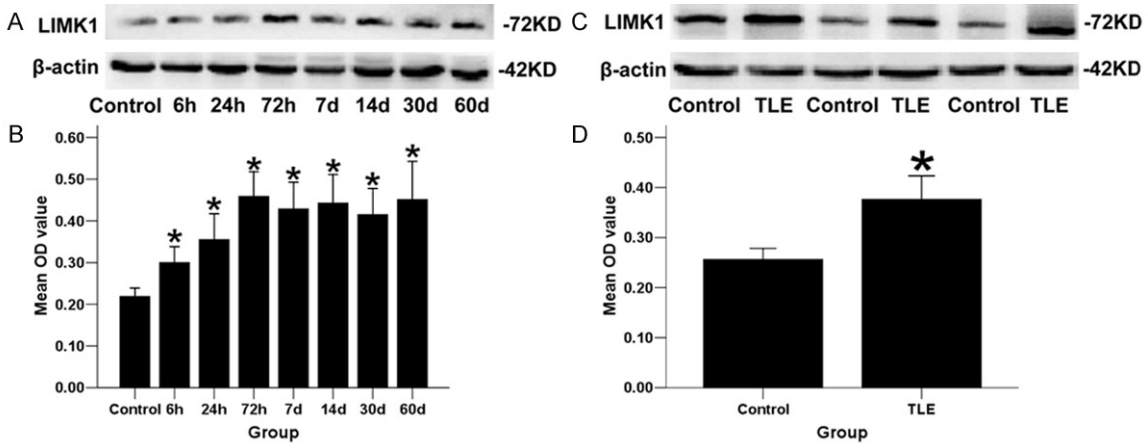

Figure 2. The LIMK1 protein was measured by Western blot assay. A. Hippocampal expression of LIMK1 following different time periods after seizures in TLE rats. B. LIMK1 protein was normalized to β-actin and compared between TLE rat subgroups and the control group. C. Representative expression of LIMK1 in TLE patients and controls. D. LIMK1 protein was normalized to β-actin and compared between TLE patients and controls. *$P < 0.05$ versus control.

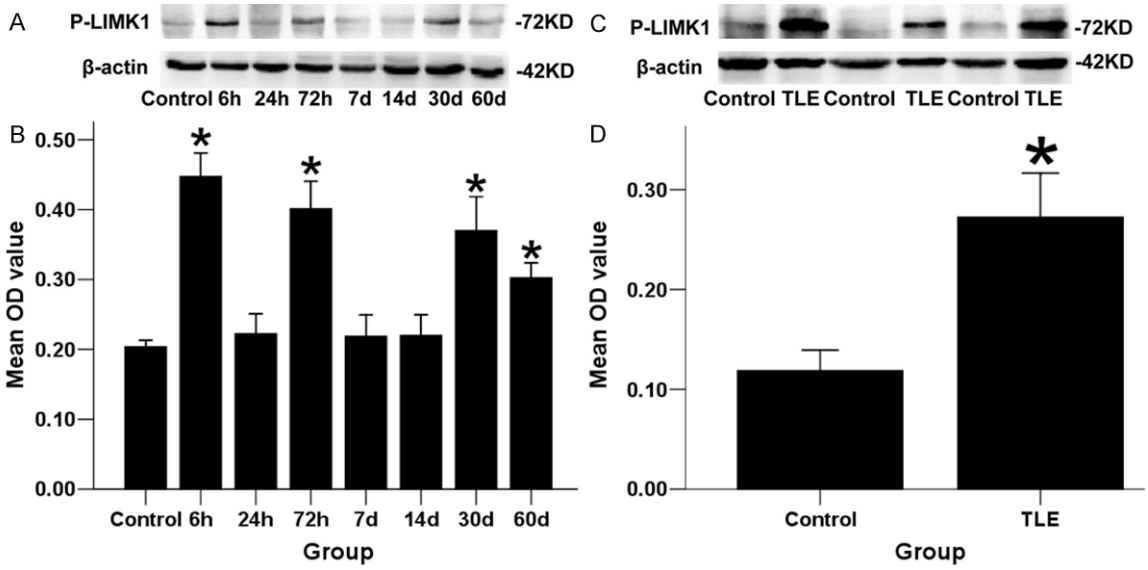

Figure 3. The p-LIMK1 protein was measured by Western blot assay. A. Hippocampal expression of p-LIMK1 following different time periods after seizures in TLE rats. B. P-LIMK1 protein was normalized to β-actin and compared between TLE rat subgroups and the control group. C. Representative expression of p-LIMK1 in intractable TLE patients and controls. D. P-LIMK1 protein was normalized to β-actin and compared between TLE patients and controls. *$P < 0.05$ versus control.

by manually counting in ten randomly selected non-overlapping high-magnification fields under a LEICA DM6000B automatic microscope.

Golgi staining

A Hito Golgi-Cox OptimStain Kit (Hitobiotec Inc. USA) was used for detecting dendrite morphology [17]. Fifteen visual fields (5 neurons per field) of every section were chosen randomly under a LEICA DM6000B automatic microscope, and the average of dendrite lengths were analyzed by the Sholl analysis [18].

Statistical analyses

Data were expressed as mean ± standard deviation (SD) and analyzed by SPSS 17.0. Student's

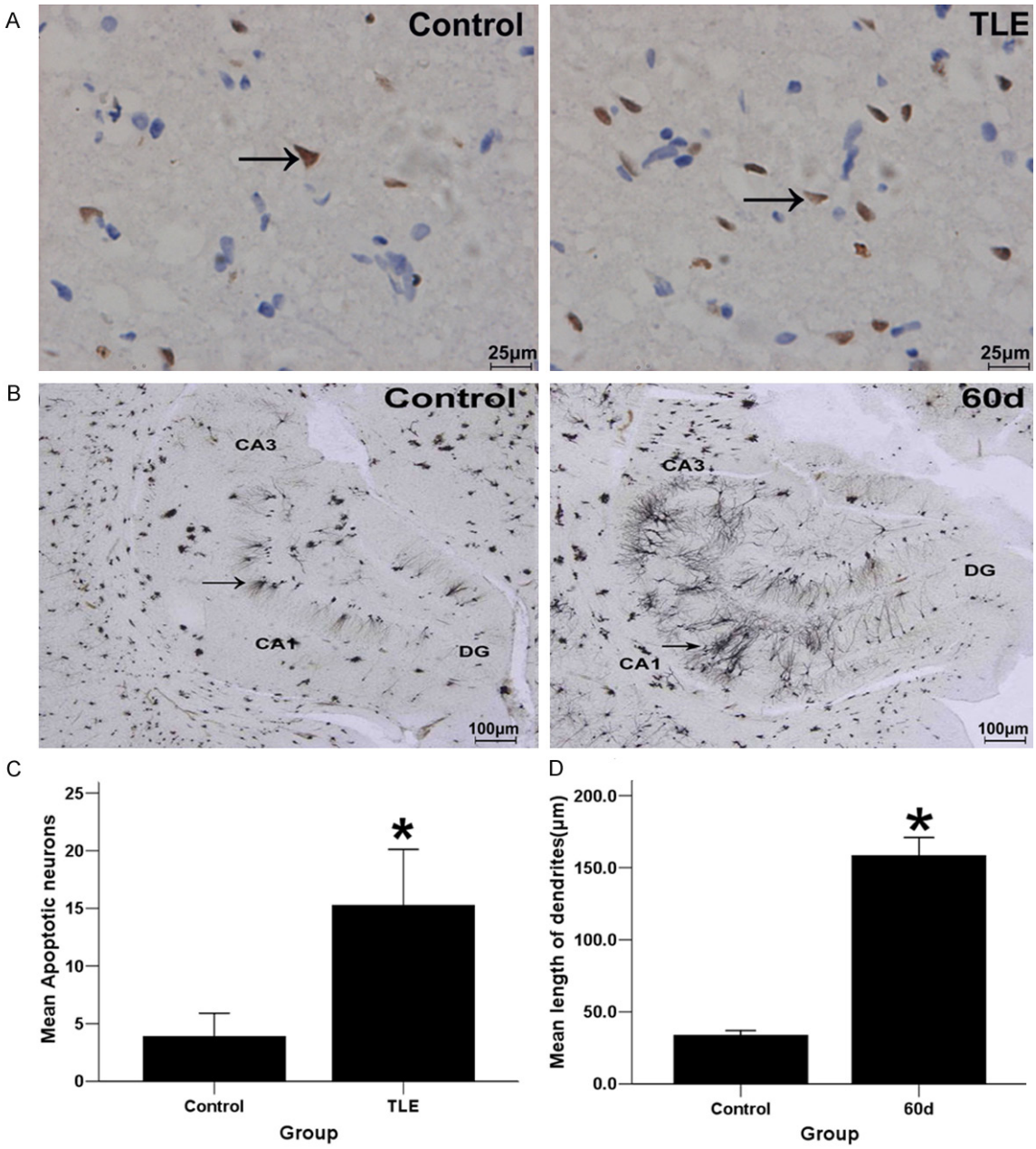

Figure 4. TUNEL staining and Golgi staining. A. Apoptotic neurons in the temporal neocortex of the patients; black arrows indicate apoptotic neurons. B. Dendrite morphology in the hippocampus; black arrows indicate dendrites. C. The number of apoptotic neurons in the temporal neocortex compared between TLE patients and controls. D. Mean dendrite length in CA1 and CA3 regions compared between TLE rat 60-day subgroup (n = 3) and control group (n = 3). *$P < 0.05$ versus control.

t-test and Chi-square test were used for comparisons between intractable TLE patients and controls. One-way ANOVA analysis was used for comparisons among groups of experimental animals, followed by Student-Newman-Keuls post hoc test. $P < 0.05$ was considered statistically significant.

Results

Clinical characteristics

The intractable TLE group was composed of 14 females and 16 males with a mean age of 26.93 ± 14.69 years, whereas the control

group was composed of 7 females and 8 males with a mean age of 26.80 ± 12.36 years. There was no significant difference in age (t = 0.03, P = 0.976) and sex (Chi-square = 0.000, P = 1.000) between TLE group and control group.

Measurement of p-LIMK1 in the hippocampus of TLE rat model by immunohistochemistry

Immunohistochemistry showed that p-LIMK1 was mainly expressed in the cytoplasm of neurons. In the hippocampi of TLE rats, compared to control group, the p-LIMK1 protein was up-regulated at 6 hours, followed by a decrease to the level of control rats at 24 hours, and up-regulated at 72 hours, then it decreased at 7 and 14 days and up-regulated at 30 and 60 days again. Besides 24 hours, 7 and 14 days, the p-LIMK1 protein expression in the hippocampi of TLE rats at the remaining post-seizure time points was significantly higher than that in control rats (P < 0.05, **Figure 1A** and **1C**). In the temporal neocortex, the intractable TLE patients exhibited significantly higher p-LIMK1 immunoreactivity than that in the control group (P < 0.05, **Figure 1B** and **1D**).

LIMK1 and p-LIMK1 protein measured by Western blot assay

The LIMK1 protein in the hippocampi of TLE rats was enhanced after seizures, and was significantly different between TLE rats and controls at each time point after seizures (P < 0.05, **Figure 2A** and **2B**). Also, the LIMK1 protein was significantly higher in TLE patients than in controls (P < 0.05, **Figure 2C** and **2D**).

The temporal expression pattern of p-LIMK1 protein in the hippocampi of TLE rats was evaluated at different times following seizures. It followed the same trend as the results of the Immunohistochemistry. The p-LIMK1 protein were significantly different between TLE rats and controls at each time point after seizures (P < 0.05), except for 24 hours, 7 and 14 days (**Figure 3A** and **3B**). The p-LIMK1 protein enhanced in intractable TLE patients compared to controls (P < 0.05, **Figure 3C** and **3D**).

Apoptotic neurons in the temporal neocortex of patients

The number of TUNEL-positive apoptotic neurons in the temporal neocortex of intractable TLE patients was significantly greater than in controls (P < 0.05, **Figure 4A** and **4C**).

Dendrite morphology in the hippocampus of rats by Golgi staining

The dendrite length in CA1 and CA3 regions of the 60-day group was significantly greater than in the control group (P < 0.05, **Figure 4B** and **4D**).

Discussion

In the CNS, changes in size, shape, structure and the number of dendritic spines have been implicated in synaptic plasticity and LTP, which are strongly correlated to the pathological basis of epilepsy [3]. Since LIMK1 plays a critical role in dendritic spine morphogenesis, synaptic plasticity and brain function [19], the expression pattern of p-LIMK1, the active form of LIMK1, in TLE patients is of great interest.

In this study, we observed up-regulation of LIMK1 and p-LIMK1 protein in TLE patients compared to controls. We speculate that the up-regulation of p-LIMK1 protein in TLE patients may be associated with phosphorylation regulation by proteins upstream of LIMK1. P-LIMK1 can phosphorylate ADF/cofilin and remodel actin filaments, which can cause the formation of excitatory loops and seizure focus [5]. At the same time, we observed the number of apoptotic neurons increased in the temporal neocortex of TLE patients. Thus, the up-regulation of p-LIMK1 protein in TLE patients may be associated with neuronal apoptosis, which was consistent with findings that activation of LIMK1 plays a role during cell apoptosis [20]. In the rat model of TLE, we found that expression of LIMK1 protein increased after seizures. However, the expression of p-LIMK1 protein fluctuated during the acute period (increased at 6 and 72 hours, decreased at 24 hours), decreased during the latent period (days 7 and 14), then increased during the chronic period (days 30 and 60). Also, we found the dendrite length in CA1 and CA3 regions increased during the chronic period (60 days). We speculate that the fluctuations in expression of p-LIMK1 during the acute period may be associated with oxidative stress induced by LiCl and pilocarpine [21] and the release of neurotransmitters due to the auto-regulation of blood-brain barrier permeability induced by pilocarpine [22]. The

down-regulation of p-LIMK1 during the latent period may be associated with alterations in growth cone formation, neuritogenesis, synaptic dysfunction, and changes in LTP in hippocampus. The up-regulation of p-LIMK1 during the chronic period might be correlated to the abnormal length of dendrites in CA1 and CA3 regions of hippocampi, resulting in the abnormal function of synaptic connections and the formation of aberrant collaterals of granule cells. This series of alterations in p-LIMK1 may result in remodeling of the cytoskeleton accompanied by changes in synaptic plasticity and LTP, and eventually leading to epilepsy.

Normal development of the CNS is dependent on the presence of LIMK1, whose deletion or mutation has been implicated in the development of the human genetic disorder Williams syndrome [23]. P-LIMK1 regulates actin cytoskeletal dynamics by inhibiting the activity of ADF/cofilins [9], and its role is closely related to synapse formation and function [19]. In the current study, the results of immunohistochemistry revealed that p-LIMK1 were expressed mainly in the cytoplasm of neurons. These data demonstrated that p-LIMK1 activity in the cytoplasm might regulate actin cytoskeletal dynamics, synaptic plasticity and LTP, which are strongly correlated to the pathology of epilepsy.

In conclusion, we confirmed that the abnormal expression of p-LIMK1 protein could be seen in TLE patients and LiCl/pilocarpine-induced TLE rats. These results indicate that p-LIMK1 might be involved in the pathogenesis of intractable TLE. The exact pathophysiological mechanism through which p-LIMK1 participates in the development of TLE, however, warrants further studies in the future.

Acknowledgements

This work was supported by a grant from the National Natural Science Foundation of China (No. 81171225). The authors sincerely thank the Xinqiao Hospital of Third Military Medical University for supplying the brain tissues used in this study, the patients and their families for their participation in this study, and the National Board of the Medical Affairs and the local ethics committee.

Disclosure of conflict of interest

None.

Address correspondence to: Dr. Yang-Mei Chen, Department of Neurology, Second Affiliated Hospital of Chongqing Medical University, 74 Lin Jiang Road, Chongqing 400010, China. Tel: (86) 13608348562; Fax: (86) 23-63693694; E-mail: chenym1997@sina.com

References

[1] Shorvon SD and Goodridge DM. Longitudinal cohort studies of the prognosis of epilepsy: contribution of the National General Practice Study of Epilepsy and other studies. Brain 2013; 136: 3497-3510.

[2] Guo D, Arnspiger S, Rensing NR and Wong M. Brief seizures cause dendritic injury. Neurobiol Dis 2012; 45: 348-355.

[3] Gardiner J and Marc J. Disruption of normal cytoskeletal dynamics may play a key role in the pathogenesis of epilepsy. Neuroscientist 2010; 16: 28-39.

[4] Scharfman HE and Gray WP. Relevance of seizure-induced neurogenesis in animal models of epilepsy to the etiology of temporal lobe epilepsy. Epilepsia 2007; 48 Suppl 2: 33-41.

[5] Williams PA, Hellier JL, White AM, Staley KJ and Dudek FE. Development of spontaneous seizures after experimental status epilepticus: implications for understanding epileptogenesis. Epilepsia 2007; 48 Suppl 5: 157-163.

[6] Proschel C, Blouin MJ, Gutowski NJ, Ludwig R and Noble M. Limk1 is predominantly expressed in neural tissues and phosphorylates serine, threonine and tyrosine residues in vitro. Oncogene 1995; 11: 1271-1281.

[7] Edwards DC, Sanders LC, Bokoch GM and Gill GN. Activation of LIM-kinase by Pak1 couples Rac/Cdc42 GTPase signalling to actin cytoskeletal dynamics. Nat Cell Biol 1999; 1: 253-259.

[8] Maekawa M, Ishizaki T, Boku S, Watanabe N, Fujita A, Iwamatsu A, Obinata T, Ohashi K, Mizuno K and Narumiya S. Signaling from Rho to the actin cytoskeleton through protein kinases ROCK and LIM-kinase. Science 1999; 285: 895-898.

[9] Arber S, Barbayannis FA, Hanser H, Schneider C, Stanyon CA, Bernard O and Caroni P. Regulation of actin dynamics through phosphorylation of cofilin by LIM-kinase. Nature 1998; 393: 805-809.

[10] Takemura M, Mishima T, Wang Y, Kasahara J, Fukunaga K, Ohashi K and Mizuno K. Ca2+/calmodulin-dependent protein kinase IV-mediated LIM kinase activation is critical for calcium signal-induced neurite outgrowth. J Biol Chem 2009; 284: 28554-28562.

[11] Eaton BA and Davis GW. LIM Kinase1 controls synaptic stability downstream of the type II BMP receptor. Neuron 2005; 47: 695-708.

[12] Fukazawa Y, Saitoh Y, Ozawa F, Ohta Y, Mizuno K and Inokuchi K. Hippocampal LTP is accompanied by enhanced F-actin content within the dendritic spine that is essential for late LTP maintenance in vivo. Neuron 2003; 38: 447-460.
[13] Guo J, Wang H, Wang Q, Chen Y and Chen S. Expression of p-CREB and activity-dependent miR-132 in temporal lobe epilepsy. Int J Clin Exp Med 2014; 7: 1297-1306.
[14] Racine RJ. Modification of seizure activity by electrical stimulation. II. Motor seizure. Electroencephalogr Clin Neurophysiol 1972; 32: 281-294.
[15] van den Brand M, Hoevenaars BM, Sigmans JH, Meijer JW, van Cleef PH, Groenen PJ, Hebeda KM and van Krieken JH. Sequential immunohistochemistry: a promising new tool for the pathology laboratory. Histopathology 2014; 65: 651-657.
[16] Giordano G and Costa LG. Measurements of neuronal apoptosis. Methods Mol Biol 2011; 758: 179-193.
[17] Das G, Reuhl K and Zhou R. The Golgi-Cox method. Methods Mol Biol 2013; 1018: 313-321.
[18] Sweet ES, Langhammer CL, Kutzing MK and Firestein BL. Semiautomated analysis of dendrite morphology in cell culture. Methods Mol Biol 2013; 1018: 261-268.
[19] Meng Y, Zhang Y, Tregoubov V, Janus C, Cruz L, Jackson M, Lu WY, MacDonald JF, Wang JY, Falls DL and Jia Z. Abnormal spine morphology and enhanced LTP in LIMK-1 knockout mice. Neuron 2002; 35: 121-133.
[20] Tomiyoshi G, Horita Y, Nishita M, Ohashi K and Mizuno K. Caspase-mediated cleavage and activation of LIM-kinase 1 and its role in apoptotic membrane blebbing. Genes Cells 2004; 9: 591-600.
[21] Freitas RM. Investigation of oxidative stress involvement in hippocampus in epilepsy model induced by pilocarpine. Neurosci Lett 2009; 462: 225-229.
[22] Nitsch C, Goping G and Klatzo I. Pathophysiological aspects of blood-brain barrier permeability in epileptic seizures. Adv Exp Med Biol 1986; 203: 175-189.
[23] Hoogenraad CC, Akhmanova A, Galjart N and De Zeeuw CI. LIMK1 and CLIP-115: linking cytoskeletal defects to Williams syndrome. Bioessays 2004; 26: 141-150.